Journal of Power Sources 195 (2010) 4700–4703

Contents lists available at ScienceDirect

Journal of Power Sources

journal homepage: www.elsevier.com/locate/jpowsour

Short communication

A novel $Ba_{0.6}Sr_{0.4}Co_{0.9}Nb_{0.1}O_{3-\delta}$ cathode for protonic solid-oxide fuel cells

Ye Lin, Ran Ran, Dengjie Chen, Zongping Shao*

State Key Laboratory of Materials-Oriented Chemical Engineering, College of Chemistry & Chemical Engineering, Nanjing University of Technology, No. 5 Xin Mofan Road, Nanjing 210009, China

ARTICLE INFO

Article history:
Received 1 February 2010
Received in revised form 21 February 2010
Accepted 22 February 2010
Available online 26 February 2010

Keywords:
Proton
Perovskite
Cathode
Solid-oxide fuel cells

ABSTRACT

$Ba_{0.6}Sr_{0.4}Co_{0.9}Nb_{0.1}O_{3-\delta}$ (BSCN), originated from $SrCo_{0.9}Nb_{0.1}O_{3-\delta}$ (SCN), is investigated as a cathode material in a protonic solid-oxide fuel cell (SOFC-H^+) with a $BaZr_{0.1}Ce_{0.7}Y_{0.2}O_3$ (BZCY) electrolyte. The surface-exchange and bulk-diffusion properties, phase reaction with the electrolyte, electrochemical activity for oxygen reduction, and performance in the real fuel cell condition of SCN and BSCN electrodes are comparatively studied by conductivity relaxation, XRD, EIS and *I–V* polarization characterizations. Much better performance is found for BSCN than SCN. Furthermore, water has a positive effect on oxygen reduction over BSCN while it has the opposite effect with SCN. A peak power density of 630 mW cm^{-2} at 700 °C is achieved for a thin-film BZCY electrolyte cell with a BSCN cathode compared to only 287 mW cm^{-2} for a similar cell with an SCN cathode. The results highly recommend BSCN as a potential cathode material for protonic SOFCs.

1. Introduction

With the growing concerns regarding increasing greenhouse-gas emissions and ever diminishing fuel reserves, solid-oxide fuel cells (SOFCs) have received considerable attention recently for their high efficiency and low emissions. Currently, particular research efforts have been paid to reducing the operating temperature of SOFCs to the intermediate-to-low temperature range of 400–650 °C for the many benefits derived from such a reduction [1]. Because state-of-the-art stabilized zirconia electrolytes have insufficient conductivity at such low operating temperatures, the development of new electrolyte becomes a necessity. Several proton-conducting oxides were found to have attractive ionic conductivity at reduced temperature, which may be even higher than the well-known doped ceria at temperatures lower than 600 °C [2–4]. Among these, $BaZr_{0.1}Ce_{0.7}Y_{0.2}O_3$ (BZCY) possesses simultaneously high conductivity and chemical stability [3].

The electrode activity is another major concern in the development of intermediate-to-low temperature SOFCs, as electrode polarization resistance usually overwhelms ohmic resistance for an SOFC with a thin-film electrolyte. During the past decade, many efforts have been made to develop innovative low temperature cathodes. Several promising cathode materials have been developed for oxygen-ionic SOFCs [5–7]. For example, perovskite-type $SrCo_{0.9}Nb_{0.1}O_{3-\delta}$ (SCN) oxide is a highly efficient cathode material for oxygen-ionic SOFCs [8]. However, the development of protonic SOFCs has been greatly retarded, with a lack of high performance cathodes to match protonic electrolytes being one of the main reasons. Simply transferring a cathode material that performs well in oxygen-ionic SOFCs to protonic SOFCs is not practicable, as the performance of an electrode is highly dependent on the electrolyte that it is fabricated on.

In this study, we report a novel $Ba_{0.6}Sr_{0.4}Co_{0.9}Nb_{0.1}O_{3-\delta}$ (BSCN) as a promising cathode material for a protonic SOFC with a BZCY electrolyte. Partial substitution of the Sr in SCN with Ba altered the effect of water on the electrode performance from detrimental to beneficial, alleviated the detrimental effect of interfacial reaction on electrolyte conductivity, and improved oxygen-bulk-diffusion and surface-exchange properties.

2. Experimental

BZCY was synthesized by an EDTA–citrate complexation process as described previously [9]. Both SCN and BSCN oxides were synthesized by a mechanoactivation-assisted solid-state reaction. The dense electrolyte for symmetric cell tests was fabricated by dry pressing and sintering at 1450 °C. The anode-supported dual-layer cells were fabricated by dual dry pressing and co-sintering at 1450 °C for 5 h. The electrodes were fabricated onto the electrolyte surface by spray deposition followed by firing in air at 1000 °C for 5 h, silver paste was used as the current collector.

The phase structure of the as-synthesized powders and products from the powder reaction were examined by X-ray diffractometry (XRD, Bruker D8 Advance).

For the electrical conductivity relaxation measurements, BSCN and SCN powders were fabricated into bar-shaped pellets by dry

* Corresponding author. Tel.: +86 25 83172256; fax: +86 25 83172256.
E-mail address: shaozp@njut.edu.cn (Z. Shao).

0378-7753/$ – see front matter.
doi:10.1016/j.jpowsour.2010.02.062

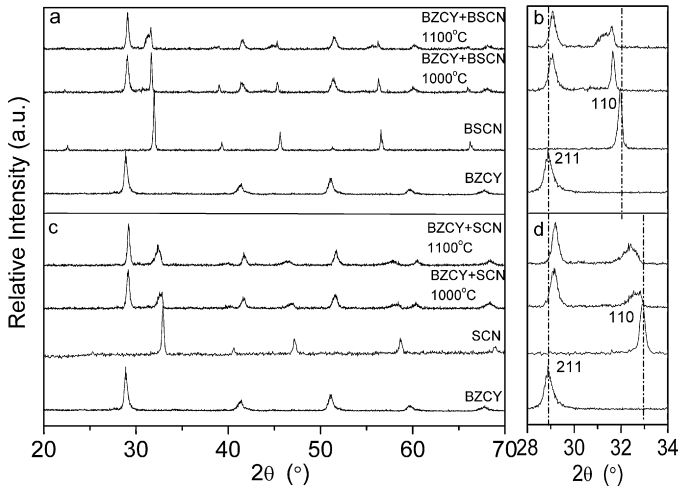

Fig. 1. XRD patterns of (a) and (b): BZCY, BSCN, and mechanically mixed BSCN + BZCY (1:1 weight ratio) composite calcined at 1000 or 1100 °C in air for 2 h; (c) and (d): BZCY, SCN, and mechanically mixed SCN + BZCY (1:1 weight ratio) composite calcined at 1000 or 1100 °C in air for 2 h.

pressing followed by sintering at 1100 °C for 5 h. The DC conductivity was measured in four-probe configuration. A constant current was supplied to the two current wires and the voltage response was recorded with a Keithley 2420 source meter.

For symmetric cell tests, electrochemical impedance spectroscopy (EIS) was measured under open-circuit voltage (OCV) conditions using an electrochemical workstation composed of a Solartron 1260A frequency–response analyzer and a Solartron 1287 potentiostat. The frequency was varied from 0.01 Hz to 100 kHz with signal amplitude of 30 mV.

For *I–V* polarization tests, a cell was sealed onto a quartz tube reactor with the cathode side exposed to ambient air while the anode was swept with humidified H_2 (3% H_2O) at a flow rate of 80 mL min^{-1} (STP). *I–V* polarization curves were collected using a Keithley 2420 digital source meter. The EIS of the cell was also measured under OCV conditions.

3. Results and discussion

Previously we demonstrated that SCN performed fairly well for oxygen reduction on a SDC electrolyte [8,10]. However, it was found that the partial substitution of the Sr^{2+} in SCN with Ba^{2+} resulted in an increase in the oxygen-permeation flux of the corresponding dense membrane at high temperature, with an optimal substitution of 60% [11]. Both oxygen-permeation through a mixed-conducting ceramic membrane and oxygen reduction over a mixed-conducting electrode in SOFCs involve the processes of oxygen-bulk-diffusion and oxygen surface-exchange. D_{chem} and k_{ex} of both BSCN and SCN were then comparatively measured using the electrical conductivity relaxation method. At 650 °C, the oxygen partial pressure of the atmosphere was suddenly changed from air to the atmosphere with oxygen partial pressure of only 0.05 atm., the electrical conductivity relaxation curves were then recorded. For a bar sample with the dimension of $2l_1$ by $2l_2$ cross-section and $2l_3$ length, with the solution of Fick's second law under appropriate initial and boundary conditions, the relative conductivity $g(t)$ with time t can be expressed as [12]:

$$g(t) = \frac{\sigma(t)-\sigma(0)}{\sigma(\infty)-\sigma(0)} = 1 - \sum_{n=1}^{\infty}\sum_{m=1}^{\infty}\sum_{p=1}^{\infty} \frac{2C_1^2 \exp(-\alpha_{1n}^2 D_{chem} t/l_1^2)}{\alpha_{1n}^2(\alpha_{1n}^2 + C_1^2 + C_1)} \times \frac{2C_2^2 \exp(-\alpha_{2m}^2 D_{chem} t/l_2^2)}{\alpha_{2m}^2(\alpha_{2m}^2 + C_2^2 + C_2)} \times \frac{2C_3^2 \exp(-\alpha_{3p}^2 D_{chem} t/l_3^2)}{\alpha_{3p}^2(\alpha_{3p}^2 + C_3^2 + C_3)} \quad (1)$$

where D_{chem} is the chemical-diffusion coefficient, $\sigma(0)$, $\sigma(t)$ and $\sigma(\infty)$ denote the initial, time dependent and final conductivities, respectively. The parameters C_1, C_2, C_3 are defined as:

$$C_1 = \frac{l_1}{L_d}, \qquad C_2 = \frac{l_2}{L_d}, \qquad C_3 = \frac{l_3}{L_d} \quad (2)$$

$$L_d = \frac{D_{chem}}{k_{ex}} \quad (3)$$

k_{ex} is the chemical surface-exchange coefficient in the relaxation process.

The coefficients a_{1n}, a_{2m} and a_{3p} are the nth, mth, pth roots, respectively, of the transcendental equations:

$$C_1 = \alpha_{1n} \tan \alpha_{1n}, \qquad C_2 = \alpha_{2m} \tan \alpha_{2m}, \qquad C_3 = \alpha_{3p} \tan \alpha_{3p} \quad (4)$$

D_{chem} and k_{ex} values were then obtained by fitting the experimental data to Eq. (1). They are 9.06×10^{-5} cm^2 s^{-1} and 2.07×10^{-3} cm s^{-1} for BSCN, respectively, while the corresponding values for SCN electrode were found to be 1.84×10^{-5} cm^2 s^{-1} and 5.68×10^{-4} cm s^{-1}, respectively. It indicates BSCN had both higher surface-exchange and higher chemical-diffusion properties than SCN.

In practical application, the electrode performance is also closely related to the interfacial properties. In fabricating an electrode

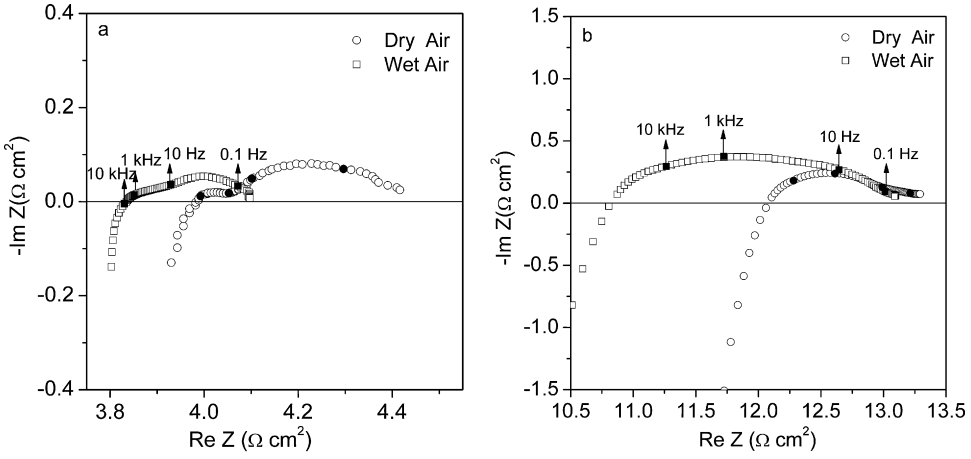

Fig. 2. AC impedance spectra of (a) BSCN and (b) SCN in dry air or wet air (~3% H_2O) at 650 °C.

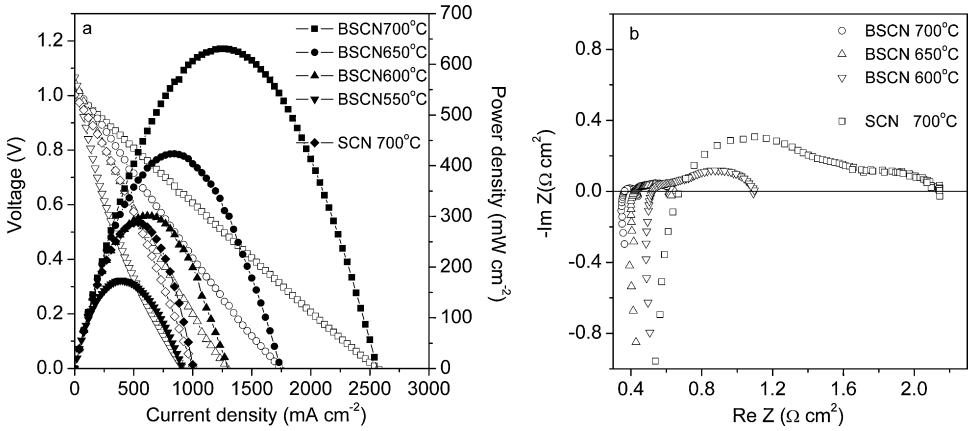

Fig. 3. (a) *I–V* and *I–P* curves of a single-cell with a BSCN or SCN cathode at various temperatures and (b) the corresponding EIS under OCV conditions.

onto an electrolyte surface, a high-temperature firing procedure is needed, which may induce an interfacial phase reaction between the two layers. The potential phase reaction between BSCN/SCN electrodes and the BZCY electrolyte was investigated by powder reaction. BSCN or SCN was mixed thoroughly with BZCY in powder form and then calcined at 1000 or 1100 °C for 5 h. As shown in Fig. 1, after the calcination, the diffraction peaks of both BSCN and SCN phases shifted to a lower angle while BZCY shifted to a higher angle. This suggests that both BSCN and SCN reacted with BZCY during the high-temperature calcination. The reaction likely involved a cation exchange between BSCN/SCN and BZCY resulting in a lattice expansion of the BSCN/SCN phases and the lattice shrinkage of the BZCY phase.

The effects of phase reaction on the electrode and electrolyte performances were investigated by EIS in a symmetric cell configuration. Shown in Fig. 2 are the typical impedance spectra of BSCN (a) and SCN (b) electrodes in Nyquist plots for symmetric cells with an electrolyte thickness of 0.65 mm. The high frequency intercept of the impedance spectrum with the real axis gives the approximate ohmic resistance of the cell (R_{ohm}), while the low-frequency intercept gives the sum of the ohmic resistance of the electrolyte and the total polarization resistance of the two symmetric electrodes ($R_{ohm} + R_p$). The difference between intercept of the impedance spectrum with the real axis at the high frequency and the low frequency can be roughly treated as the electrode polarization resistance (here, the values have been divided by two). The results indicated that the cell with SCN electrodes had a much larger ohmic resistance than with BSCN. In dry air at 650 °C, the resistances were ~4.0 and ~12.0 Ω cm^2 for the cells with BSCN and SCN electrodes, respectively. Such a large difference is clearly related to the phase reaction between the electrode and the electrolyte. In other words, the phase reaction between BSCN and BZCY had much less effect on the ionic conductivity of the BZCY electrolyte than that between SCN and BZCY. The BSCN electrode also showed a smaller polarization resistance (~0.4 Ω cm^2) than SCN (~1.2 Ω cm^2) at 650 °C, which can be attributed in part to the better surface-exchange and chemical-diffusion properties of BSCN versus SCN.

An important difference from an oxygen-ionic SOFC is that water in a protonic SOFC is produced at the cathode side. The effect of water on cathode performance is therefore of great concern in protonic SOFCs. To evaluate this effect, the symmetric cells were also operated in a 3%-H_2O-humidified air atmosphere. As shown in Fig. 2, a modest reduction in electrolyte ohmic resistance was observed compared to that measured in dry air. Actually, the contribution of p-type electronic conduction may decrease and proton conduction will appear while water vapor is introduced to dry air for $Ba_xCe_{0.9}Y_{0.1}O_{3-\delta}$ (x = 1.05, 0.95) [13], in this case, it seemed that the introduced proton conductivity is larger than the decreased p-type electronic conductivity for the bulk of the electrolyte in the symmetric cells. However, a very different effect on the electrode performance was observed for the BSCN and SCN electrodes. The R_p for BSCN decreased from 0.44 Ω cm^2 in dry air to 0.27 Ω cm^2 with the introduction of water vapor at 650 °C, while the R_p of SCN increased substantially, from 1.22 Ω cm^2 in dry air to 2.23 Ω cm^2 in humidified air. This further demonstrates that BSCN is far superior to SCN as a cathode in protonic SOFCs.

To determine its performance in real fuel cell conditions, complete cells with BSCN cathodes were fabricated. Shown in Fig. 3a are the *I–V* curves of the cells with BSCN cathodes and thin-film BZCY electrolytes (~30 μm), and, for comparison, the results of similar cells with SCN cathodes. The cells with BSCN cathodes showed a relatively high performance of 630 mW cm^{-2} at 700 °C, which is among the highest performance of protonic SOFCs reported in the available literature, for example, a peak power density of 725 mW cm^{-2} was achieved at 700 °C by Yang et al. [14] with a composite cathode of BZCY and $Sm_{0.5}Sr_{0.5}CoO_{3-\delta}$ (SSC). Very recently, a peak power density of 665 mW cm^{-2} at 700 °C was also reported by Sun et al. [15] using a composite cathode of SSC and SDC. It implies that the formation of composite cathode of BSCN and BZCY or SDC may further increase the electrode performance of BSCN cathode. However, the cells with SCN as the cathode showed a peak power density of only 287 mW cm^{-2} under similar conditions. As both cells had a similar OCV of ~1.0 V at 700 °C, the major difference of the single-cell performance was likely due to their different cell resistances. Shown in Fig. 3b are the corresponding impedance spectra of the cells with BSCN cathodes under OCV conditions, and, for comparison, the impedance spectra of the corresponding SCN cells at 700 °C. The intercept with real axis at high frequency represents the electrolyte resistance (R_s) of cell and the other intercept at low frequency corresponds to the total resistance (R_t) of cell. Thus, the interfacial resistance (R_p) of cell was considered as the difference between Rt and R_s. The R_p values of the cells with BSCN cathodes were 0.06, 0.23 and 0.57 Ω cm^2, respectively, at 700, 650 and 600 °C, these results were also compared with several literature reports, for example, the polarization resistances of cells with BZCY–LSCF cathode are estimated to be about 0.19, 0.47, 1.34 Ω cm^2 at 650, 600, and 550 °C, respectively [16], a cell polarization resistance of 0.08 and 0.8 Ω cm^{-2} were observed at 700 and 600 °C with a single $SmBa_{0.5}Sr_{0.5}Co_2O_{5+\delta}$ cathode [17]. The cells with SCN cathodes suffered from much larger R_s and R_p than similar cells with BSCN cathodes. Fig. 4 shows the SEM photo of the cell with BSCN cathode after the *I–V* polarization test from across-sectional view. It is worth pointing out that the I–V curves are almost linear implying

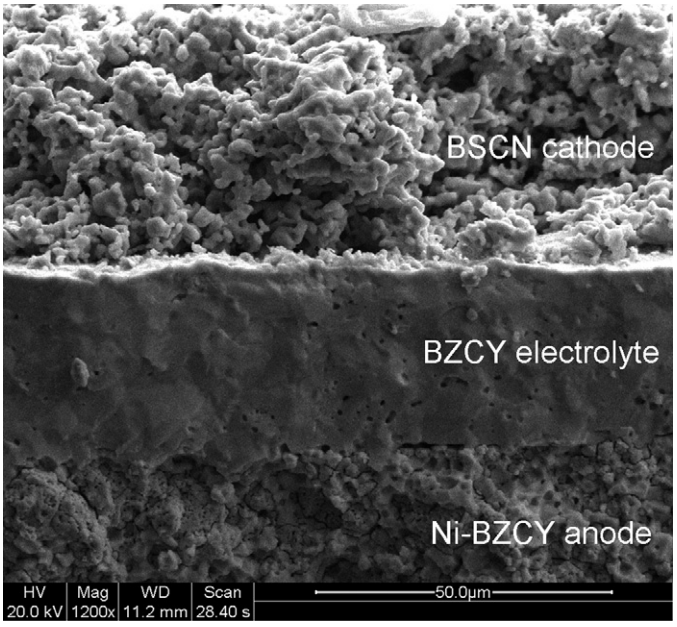

Fig. 4. SEM image from a cross-sectional view of the cell with BSCN cathode after the *I–V* polarization tests.

that there are a little activation loss and concentration polarization loss mainly related to the high catalytic activity of BSCN cathode and sufficient porosity of Ni-BZCY anode. After the fuel cell test, the cathode still adhered to the electrolyte surface without evidence for delimitation. This suggests that the BSCN cathode matched the BZCY electrolyte well during the test.

4. Conclusions

BSCN had improved surface-exchange and bulk-chemical-diffusion properties over SCN. Although there were phase reactions, likely involving cation exchange, of both the BSCN and the SCN electrodes with the BZCY electrolyte at high temperature, the effects on electrolyte conductivity were much less with BSCN than with SCN. As a result, symmetric cells with BSCN cathodes showed both smaller cell ohmic resistance and electrode polarization resistance than similar cells with SCN electrodes. The positive effect of water on the oxygen reduction over BSCN electrodes is another significant advantage of BSCN over SCN as a cathode in a protonic SOFC. As a result, much higher cell performance was observed for the cells with BSCN electrodes than with SCN electrodes. A peak power density of 630 mW cm^{-2} and an electrode polarization resistance of 0.06 $\Omega\,cm^2$ were achieved for a cell with a BSCN electrode at 700 °C. These results indicate that BSCN is a highly promising cathode material for protonic SOFCs.

Acknowledgements

This work was supported by the National Natural Science Foundation of China under Contract Nos. 20646002, 20676061 and 20703024, by the National 863 program under Contract No. 2007AA05Z133, and by the National Basic Research Program of China under Contract No. 2007CB209704.

References

[1] B.C.H. Steele, A. Heinzel, Nature 414 (2001) 345–352.
[2] K.D. Kreuer, Annu. Rev. Mater. Res. 33 (2003) 333–359.
[3] C.D. Zou, S.W. Zha, M.L. Liu, M. Hatano, M. Uchiyama, Adv. Mater. 18 (2006) 3318–3320.
[4] L. Yang, S.Z. Wang, K. Blinn, M.F. Liu, Z. Liu, Z. Cheng, M.L. Liu, Science 326 (2009) 126–129.
[5] Z.P. Shao, S.M. Haile, Nature 431 (2004) 170–173.
[6] W. Zhou, R. Ran, Z.P. Shao, J. Power Sources 192 (2009) 231–246.
[7] J.M. Vohs, R.G. Gorte, Adv. Mater. 21 (2009) 943–956.
[8] W. Zhou, Z.P. Shao, R. Ran, W.Q. Jin, N.P. Xu, Chem. Commun. 44 (2008) 5791–5793.
[9] Y. Lin, R. Ran, Y. Zheng, Z.P. Shao, W.Q. Jin, N.P. Xu, J.M. Ahn, J. Power Sources 180 (2009) 15–22.
[10] W. Zhou, W.Q. Jin, Z.H. Zhu, Z.P. Shao, Int. J. Hydrogen Energy 35 (2010) 1356–1366.
[11] J. Zhao, K. Zhang, D.M. Gao, Z.P. Shao, S.M. Liu, Sep. Sci. Technol. 71 (2010) 152–159.
[12] I. Yasuda, M. Hishinuma, J. Solid State Chem. 123 (1996) 382–390.
[13] G.L. Ma, T. Shimura, H. Iwahara, Solid State Ionics 110 (1998) 103–110.
[14] L. Yang, C.D. Zuo, S.Z. Wang, Z. Cheng, M.L. Liu, Adv. Mater. 20 (2008) 3280–3283.
[15] W.P. Sun, L.T. Yan, B. Lin, S.Q. Zhang, W. Liu, J. Power Sources 195 (2010) 3155–3158.
[16] L. Yang, Z. Liu, S.Z. Wang, Y.M. Choi, C.D. Zuo, M.L. Liu, J. Power Sources 195 (2010) 471–474.
[17] H.P. Ding, X.J. Xue, X.Q. Liu, G.Y. Meng, J. Power Sources 195 (2010) 775–778.